HHS Public Access

Author manuscript

Doc Ophthalmol. Author manuscript; available in PMC 2019 April 01.

Published in final edited form as:

Doc Ophthalmol. 2018 April ; 136(2): 125–133. doi:10.1007/s10633-018-9626-1.

Phenotypic Expansion and Progression of *SPATA7*-associated Retinitis Pigmentosa

Jesse D. Sengillo, B.S.[1,2,3], **Winston Lee, M.A.**[2], **Colleen G. Bilancia, Ph.D.**[4], **Vaidehi Jobanputra, PhD, FACMG**[4], and **Stephen H. Tsang, M.D., Ph.D.**[1,2,4,5,§]

[1]Jonas Children's Vision Care, and Bernard & Shirlee Brown Glaucoma Laboratory

[2]Department of Ophthalmology, Columbia University, New York, NY, USA

[3]State University of New York Downstate Medical Center, Brooklyn, NY, USA

[4]Department of Pathology & Cell Biology, Columbia University Medical Center, New York, NY, USA

[5]Institute of Human Nutrition, College of Physicians and Surgeons, Columbia University, New York, NY, USA

Abstract

Purpose—To report an unusual phenotype of retinitis pigmentosa caused by compound heterozygous mutations in *SPATA7*, and describe the progression over a two-year follow-up period.

Methods—Retrospective case study.

Results—A 63-year-old man with a long history of nyctalopia, progressive visual field constriction, and a recent subacute decrease in visual acuity of the left eye presented for evaluation of a suspected retinal degeneration. Multi-modal retinal imaging and functional assessment with full-field electroretinogram suggested a severe rod-cone dysfunction masquerading as a choroideremia-like phenotype. A vitreous opacity was found to explain recent changes in the left eye and a 25-guage vitrectomy and membrane peel was performed, yielding no change in visual acuity. Whole exome sequencing revealed compound heterozygous variants in *SPATA7* that were predicted to be pathogenic.

[§]Address Correspondence: Stephen H. Tsang, MD, PhD, Harkness Eye Institute, 635 West 165th Street, Box 212, New York, NY 10032, Phone: (212) 342-1189/Fax: 212-305-4987/ sht2@columbia.edu.

COMPLIANCE WITH ETHICAL STANDARDS

Conflicts of interest: The authors declare that they have no conflicts of interest.

Informed consent: The data presented in this study, including images and genetic testing results, are not identifiable to individual patients. For this type of study, formal consent is not required.

Ethics approval: All procedures performed in studies involving human participants were in accordance with the ethical standards of the institutional and/or national research committee and with the 1964 Helsinki declaration and its later amendments or comparable ethical standards.

AUTHOR CONTRIBUTIONS

J.D.S and W.L. collected and interpreted patient data and images, and composed the manuscript. C.G.B. and V.J. performed and interpreted genetic analyses. S.H.T. conceived the experimental design and approved the final interpretation of the data.

Conclusions—Compound heterozygous c.1100A>G, p.(Y367C) and c.1102_1103delCT, p.(L368Efs*4) variants in *SPATA7* manifest as an unusual RP phenotype in this case, showing extensive choroidal sclerosis and RPE atrophy with evidence of progression over two years on multi-modal imaging.

Keywords

SPATA7; retinitis pigmentosa; choroidal sclerosis

INTRODUCTION

Retinitis pigmentosa (RP, OMIM# 268000) is a rare inherited retinal dystrophy that causes progressive and irreversible blindness, having significant impact on daily function of affected patients [1–4]. Mutations in over 70 genes are known to cause RP, however the phenotype can be quite variable depending on the underlying genetic etiology. In fact, patients with pathogenic mutations in the same gene may manifest as a different clinical entity [5]. Examples include genes associated with more than one presentation, such as RP or Leber congenital amaurosis (LCA): *CEP290*, *CRB1*, *CRX*, *IFT140*, *IMPDH1*, *IQCB1*, *LRAT*, *PRPH2*, *RDH12*, *RPE65*, *RPGRIP1*, *SPATA7*, and *TULP1* (RetNet, https://sph.uth.edu/retnet, accessed January 2018).

SPATA7, or spermatogenesis associated 7 gene, is expressed in the retina along with other tissue such as the testis, where it was first identified [6]. It is a ciliopathy gene that encodes a product required for correct cellular translocation of RPGRIP1 protein in the retina [7]. Normal SPATA7 interacts with microtubules of the photoreceptor cilium and binds the coiled-coil domain of RPGRIP1. In *Spata7*$^{-/-}$ mice, mislocalization of RPGRIP1 and rhodopsin to the inner segment is observed, leading to decreased responsiveness to light under scotopic conditions and retinal degeneration [7]. When this mouse model is treated with subretinal *Spata7* cDNA via an adeno-associated viral vector, AAV8, the degeneration is alleviated at early stages [8].

Only a few studies have sought to assess genotype-phenotype relationships for *SPATA7*-associated retinal degeneration [9–12], identifying that patients can present as either a juvenile RP or LCA phenotype. In this case study, we identify the first case of a patient with biallelic mutations in *SPATA7* presenting with severe choroidal sclerosis and RPE atrophy, largely resembling a choroideremia-like fundus on multimodal imaging.

CASE STUDY

An otherwise healthy 63-year-old man presented for evaluation of presumed retinitis pigmentosa that was diagnosed at 31 years of age. In addition to progressive nyctalopia, visual field constriction, and a decrease in visual acuity since diagnosis, the patient reported a recent, rapid decline of visual acuity in the left eye accompanying a recent halo-effect around objects. Ocular history included cataract surgery and subsequent Yag laser capsulotomy four years prior in both eyes. There was no other family member with a history of similar vision loss. At the time of presentation, the patient was taking supplemental vitamin A and lutein.

Vision was best corrected to 20/30 and 20/60 in the right and left eyes respectively, with plano refraction bilaterally. Slit-lamp examination revealed an unremarkable anterior chamber and iris, with each eye containing a posterior chamber intraocular lens that was well-positioned. Dilated fundus exam revealed extensive chorioretinal degeneration of the peripheral retina, progressing towards the central macula which contained triangular-shaped islands of spared retinal pigment epithelium (RPE) in each eye. A similar, but smaller, spared region of RPE was present nasal to the discs in both eyes. Extensive intraretinal pigment migration was present along the mid-periphery (Fig. 1A and B). A dense opacity noted in the vitreous of the left eye was consistent with a floater obstructing the visual axis.

Short-wavelength fundus autofluorescence (FAF) and spectral-domain optical coherence tomography (SD-OCT) were obtained (Spectralis HRA + OCT device; Heidelberg Engineering, Heidelberg, Germany). FAF imaging revealed widespread, continuous loss of RPE encroaching on the central macula in both eyes (Fig. 1C and 1D). The degenerative boundaries between spared and affected RPE appeared sharp. The parafoveal region of each eye appeared to have a relatively increased area of hyperautofluorescence. SD-OCT corroborated findings seen on FAF imaging and fundoscopy (Fig. 2). Extensive degeneration and sclerosis of the choroid was evident in areas of RPE loss. Areas with RPE loss showed increased transmittance of signal to the choroidal and scleral layers. Enhanced depth imaging on SD-OCT revealed an abrupt thinning of the underlying choroidal layer in areas of atrophy adjacent to the region of spared RPE. An outer retinal tubulation (ORT) was present temporally in the right eye (Fig. 2, yellow arrowhead). Focal areas of RPE thickening were present, and more prominent in the right eye (Fig. 2, green arrowheads). Full-field electroretinography (ffERG) revealed completely extinguished scotopic and photopic responses using Dawson, Trick, and Litzkow (DTL)-recording electrodes and Ganzfeld stimulation according to international standards as outlined by the International Society for Clinical Electrophysiology of Vision (ISCEV) (Fig. 3) [13,14]. Burian-Allen (BA) electrodes were subsequently utilized under photopic conditions to detect potential residual cone function, however the 30 Hz-flicker amplitudes remained undetectable at less than 0.1μv in both eyes.

Given the asymmetrical progression reported by the patient, which was noticed in the left eye for the last eight months, and a dense opacity in the left vitreous noted on exam to be obstructing the remaining central island left in his vision, the decision was made to remove the opacity by 25-guage vitrectomy, endolaser focal photocoagulation, and air-fluid exchange surgery. During the surgery, a small membrane was also noted to be overlying the posterior pole of the central island. This was stained with intravitreal kenalog and peeled from the macula. No tears or leakage were noted at the end of surgery and the vitreous was filled with a gas bubble, with the retina appearing completely flat. Dilated fundus exam of the left eye showed clear vitreous and a spared central island which was previously less discernable.

The patient returned to clinic for routine follow-up two years later and reported no subsequent changes in vision. Best corrected visual acuity was 20/25 in the right and 20/60 in the left. Dilated fundus exam was unchanged from the post-surgery visit two years prior. On SD-OCT, the previous ORT seen in the temporal macula of the right eye was now absent

with the corresponding area showing RPE atrophy, increased choroidal sclerosis, and transmittance of signal to the sclera (Fig. 4). FAF confirmed a reduction in the area of centrally spared RPE as compared to its appearance at baseline, bilaterally (OD, −4.4mm^2; OS, −3.8mm^2) (Fig. 5).

Clinical whole exome sequencing was performed at the Laboratory of Personalized Genomic Medicine at Columbia University Medical Center. Specifically, DNA was extracted from the peripheral blood of the patient, a DNA library was prepared using Agilent SureSelectXT Human All Exon V5+UTRs capture, and sequencing was performed using Illumina HiSeq2500 sequencing technology. Patient data was aligned to the reference genome and analyzed for genetic variants using NextGENe software from Softgenetics. Results were filtered with an in-house proprietary analytical pipeline and variants of interest were analyzed using the ACMG classification guideline [15]. The reported variants were also confirmed by Sanger sequencing in the clinical lab. The analysis revealed two variants in *SPATA7*. One mutation was a novel missense variant c.1100A>G, which results in the substitution of the highly conserved Tyr variant with Cys, p.(Tyr367Cys) (phyloP: 6.81). *In silico* prediction algorithms were used to assess the Tyr367Cys missense substitution. Predictions are based on the evolutionary conservation of the sequence (phyloP), the conservation between the biochemical properties of the two amino acids (SIFT, Grantham score, AlignGVGD), or a combination of these along with other reported information about the variant such as population frequency (MutationTaster). These *in silico* predictors support the deleterious nature of this missense change (phyloP: 3.203 score range: −14 to +6 with positive scores indicating a conserved position; SIFT score: 0, range 0–1 with damaging being <0.05; Grantham score: 194, score range: 5–215 with high scores indicating damaging changes; AlignGVGD score: class 0, least likely to be damaging; MutationTaster: disease-causing). A previously reported two base pair deletion was also identified in *SPATA7*, c. 1102_1103delCT, resulting in a frameshift at exon 10, p.(Leu368Glufs*4) [16]. The resulting new reading frame terminates three positions downstream and the mRNA transcript produced is targeted for nonsense mediated decay. Minor allele frequencies of the missense and deletion variants were both under 0.00003% in the heterozygous state with no homozygotes in 123,136 exome sequences and 15,496 whole-genome sequences, according to the Genome Aggregation Database (gnomAD) (http://gnomad.broadinstitute.org; accessed January 2018). Co-segregation analysis was performed in an unaffected family member, confirming the variants to be in trans.

DISCUSSION

To the authors' knowledge, this is the first case of *SPATA7*-RP presenting with prominent RPE atrophy and choroidal sclerosis, expanding the phenotypic and mutational spectrum. Wang et al. previously compared families with *SPATA7*-associated retinal degeneration [11]. One family manifesting as the more severe phenotype (LCA), had nonsense mutations located in exons 5 and 8. Juvenile onset RP patients had later occurring mutations in the last two exons of the gene, closer to the C-terminus. Another study had similar findings when assessing the location of *SPATA7* mutations in LCA patients [10]. Our patient had compound heterozygous mutations, both occurring in exon 10 (of 12), supporting the notion that mutations occurring in later exons may tend towards an RP phenotype. One mutation

identified in this patient was novel. The c.1100A>G is predicted to change residue 367 from tyrosine to cysteine. *In silico* analyses generally predicted this change to be deleterious and damaging to protein structure and function. The c.1102_1103delCT variant was identified on the opposite allele and predicted to cause a frameshift at residue 368, subsequently resulting in a premature stop codon three positions downstream of the deletion.

The patient was clinically diagnosed with RP as opposed to LCA, as he did not have a history of nystagmus, amaurotic pupils, or childhood onset blindness. Of note, a severe RP phenotype was seen on ffERG with nondetectable 30 Hz-flicker responses using DTL-recording electrodes and less than 0.1μv bilaterally with BA contact lens electrodes. Greater than 0.5μV is generally regarded as the voltage needed for 'useful vision' [17]. Progression was also detectable over the follow-up period on FAF and SD-OCT. However, the patient maintained a visual acuity of 20/30 and 20/60 in the right and left eyes, respectively, over a two-year follow-up period. Preserved acuity in this region is likely attributable to functioning foveal cones.

In the present case, vitrectomy was performed for several reasons, including the subacute change in subjective visual acuity of the left eye reported by the patient, asymmetry in BCVA, and the presence of a left vitreous opacity on exam. Post-operative assessment revealed that the opacity was successfully removed without complication and the visual axis overlying the spared RPE island was optically clear. However, BCVA remained unchanged after vitrectomy and membrane peeling, highlighting the importance of pre-surgical counseling in patients with retinitis pigmentosa, as the contribution of non-retinal pathology to vision loss can be difficult to estimate and thus alter patient expectation. Similar practice is used in the assessing RP patients for cataract extraction as recommendations are best made a on a case-by-case basis [18].

Unique to this patient, a choroideremia-like phenotype was observed. In choroideremia (CHM, OMIM 303100), an X-linked inherited retinal dystrophy, there is a pronounced RPE phenotype, as the defective gene results in build-up of unprenylated Rab proteins in the RPE [2]. In this condition, there is extensive RPE and choroidal degeneration down to the sclera, yielding a pale appearing fundus,[19] similar to our patient. Furthermore, on FAF imaging in CHM and our patient, sharp edges can be seen at the boundary of spared and degenerated RPE. Candidate gene testing was not performed to rule out CHM initially, as the family history was less consistent with X-linked inheritance (no affected males on the maternal side, but rather an autosomal recessive mode of inheritance) and there was extensive intraretinal pigment migration, which is seen more commonly in photoreceptor-predominant pathologies in our experience. At present, the relationship between SPATA7 dysfunction and a severe choroidal phenotype in our patient remains elusive. A previous study localized SPATA7 function to the ganglion cell layer, inner nuclear layer, and inner segment of photoreceptors in young mice [11], whereas Eblimit et al. found this gene critical for protein trafficking in photoreceptor cilia [7]. In hTERT RPE-1 cells, SPATA7 localized with the cellular microtubule network and to the ciliary axoneme in ciliated cells [7]. Diseased RPE may lead to loss of choroidal fenestration and a subsequent choroideremia-like phenotype. Alternatively, the effect on the choroid could be explained in part by other unidentified genetic modifiers. Supporting the latter includes another case of choroideremia-like RP

associated with a different ciliopathy gene, namely *RP2* which encodes a protein that regulates ciliary tip kinesins [20]. Future studies are needed to discern whether the phenotype seen in our study is unique to the combination of the two-identified compound heterozygous variants and potential modifiers, or simply a phenotypic subset of *SPATA7*-associated retinal degeneration in general.

Acknowledgments

FUNDING

Jonas Children's Vision Care, and Bernard & Shirlee Brown Glaucoma Laboratory are supported by the National Institutes of Health [5P30EY019007, R01EY018213, R01EY024698, R01EY026682, R21AG050437], National Cancer Institute Core [5P30CA013696], the Research to Prevent Blindness (RPB) Physician-Scientist Award, unrestricted funds from RPB, New York, NY, USA. J.D.S is supported by the RPB Medical Student Eye Research Fellowship. S.H.T. is a member of the RD-CURE Consortium and is supported by the Tistou and Charlotte Kerstan Foundation, the Schneeweiss Stem Cell Fund, New York State [C029572], the Foundation Fighting Blindness New York Regional Research Center Grant [C-NY05-0705-0312], the Crowley Family Fund, and the Gebroe Family Foundation.

References

1. Sengillo JD, Justus S, Cabral T, Tsang SH. Correction of Monogenic and Common Retinal Disorders with Gene Therapy. Genes (Basel). 2017; 8(2)doi: 10.3390/genes8020053
2. Sengillo JD, Justus S, Tsai YT, Cabral T, Tsang SH. Gene and cell-based therapies for inherited retinal disorders: An update. Am J Med Genet C Semin Med Genet. 2016; 172(4):349–366. DOI: 10.1002/ajmg.c.31534 [PubMed: 27862925]
3. Berson EL. Retinitis pigmentosa. The Friedenwald Lecture. Invest Ophthalmol Vis Sci. 1993; 34(5): 1659–1676. [PubMed: 8473105]
4. Hamel C. Retinitis pigmentosa. Orphanet J Rare Dis. 2006; 1:40.doi: 10.1186/1750-1172-1-40 [PubMed: 17032466]
5. Broadgate S, Yu J, Downes SM, Halford S. Unravelling the genetics of inherited retinal dystrophies: Past, present and future. Prog Retin Eye Res. 2017; doi: 10.1016/j.preteyeres.2017.03.003
6. Zhang X, Liu H, Zhang Y, Qiao Y, Miao S, Wang L, Zhang J, Zong S, Koide SS. A novel gene, RSD-3/HSD-3.1, encodes a meiotic-related protein expressed in rat and human testis. J Mol Med (Berl). 2003; 81(6):380–387. DOI: 10.1007/s00109-003-0434-y [PubMed: 12736779]
7. Eblimit A, Nguyen TM, Chen Y, Esteve-Rudd J, Zhong H, Letteboer S, Van Reeuwijk J, Simons DL, Ding Q, Wu KM, Li Y, Van Beersum S, Moayedi Y, Xu H, Pickard P, Wang K, Gan L, Wu SM, Williams DS, Mardon G, Roepman R, Chen R. Spata7 is a retinal ciliopathy gene critical for correct RPGRIP1 localization and protein trafficking in the retina. Hum Mol Genet. 2015; 24(6):1584–1601. DOI: 10.1093/hmg/ddu573 [PubMed: 25398945]
8. Zhong H, Eblimit A, Moayedi Y, Boye SL, Chiodo VA, Chen Y, Li Y, Nichols RM, Hauswirth WW, Chen R, Mardon G. AAV8(Y733F)-mediated gene therapy in a Spata7 knockout mouse model of Leber congenital amaurosis and retinitis pigmentosa. Gene Ther. 2015; 22(8):619–627. DOI: 10.1038/gt.2015.42 [PubMed: 25965394]
9. Mackay DS, Ocaka LA, Borman AD, Sergouniotis PI, Henderson RH, Moradi P, Robson AG, Thompson DA, Webster AR, Moore AT. Screening of SPATA7 in patients with Leber congenital amaurosis and severe childhood-onset retinal dystrophy reveals disease-causing mutations. Invest Ophthalmol Vis Sci. 2011; 52(6):3032–3038. DOI: 10.1167/iovs.10-7025 [PubMed: 21310915]
10. Perrault I, Hanein S, Gerard X, Delphin N, Fares-Taie L, Gerber S, Pelletier V, Merce E, Dollfus H, Puech B, Defoort-Dhellemmes S, Petersen MD, Zafeiriou D, Munnich A, Kaplan J, Roche O, Rozet JM. Spectrum of SPATA7 mutations in Leber congenital amaurosis and delineation of the associated phenotype. Hum Mutat. 2010; 31(3):E1241–1250. DOI: 10.1002/humu.21203 [PubMed: 20104588]
11. Wang H, den Hollander AI, Moayedi Y, Abulimiti A, Li Y, Collin RW, Hoyng CB, Lopez I, Abboud EB, Al-Rajhi AA, Bray M, Lewis RA, Lupski JR, Mardon G, Koenekoop RK, Chen R.

Mutations in SPATA7 cause Leber congenital amaurosis and juvenile retinitis pigmentosa. Am J Hum Genet. 2009; 84(3):380–387. DOI: 10.1016/j.ajhg.2009.02.005 [PubMed: 19268277]

12. Mayer AK, Mahajnah M, Zobor D, Bonin M, Sharkia R, Wissinger B. Novel homozygous large deletion including the 5′ part of the SPATA7 gene in a consanguineous Israeli Muslim Arab family. Mol Vis. 2015; 21:306–315. [PubMed: 25814828]
13. McCulloch DL, Marmor MF, Brigell MG, Hamilton R, Holder GE, Tzekov R, Bach M. Erratum to: ISCEV Standard for full-field clinical electroretinography (2015 update). Doc Ophthalmol. 2015; 131(1):81–83. DOI: 10.1007/s10633-015-9504-z [PubMed: 26059396]
14. McCulloch DL, Marmor MF, Brigell MG, Hamilton R, Holder GE, Tzekov R, Bach M. ISCEV Standard for full-field clinical electroretinography (2015 update). Doc Ophthalmol. 2015; 130(1): 1–12. DOI: 10.1007/s10633-014-9473-7
15. Richards S, Aziz N, Bale S, Bick D, Das S, Gastier-Foster J, Grody WW, Hegde M, Lyon E, Spector E, Voelkerding K, Rehm HL, ACMG Laboratory Quality Assurance Committee. Standards and guidelines for the interpretation of sequence variants: a joint consensus recommendation of the American College of Medical Genetics and Genomics and the Association for Molecular Pathology. Genet Med. 2015; 17(5):405–24. DOI: 10.1038/gim.2015.30 [PubMed: 25741868]
16. Consugar MB, Navarro-Gomez D, Place EM, Bujakowska KM, Sousa ME, Fonseca-Kelly ZD, Taub DG, Janessian M, Wang DY, Au ED, Sims KB, Sweetser DA, Fulton AB, Liu Q, Wiggs JL, Gai X, Pierce EA. Panel-based Genetic Diagnostic Testing for Inherited Eye Diseases is Highly Accurate and Reproducible and More Sensitive for Variant Detection Than Exome Sequencing. Genet Med. 2015; 17(4):253–261. DOI: 10.1038/gim.2014.172 [PubMed: 25412400]
17. Berson EL. Long-term visual prognoses in patients with retinitis pigmentosa: the Ludwig von Sallmann lecture. Exp Eye Res. 2007; 85(1):7–14. DOI: 10.1016/j.exer.2007.03.001 [PubMed: 17531222]
18. Parmeggiani F, Sato G, De Nadai K, Romano MR, Binotto A, Costagliola C. Clinical and Rehabilitative Management of Retinitis Pigmentosa: Up-to-Date. Curr Genomics. 2011; 12(4): 250–259. DOI: 10.2174/138920211795860125 [PubMed: 22131870]
19. Ma KK, Lin J, Boudreault K, Chen RW, Tsang SH. Phenotyping Choroideremia and Its Carrier State with Multimodal Imaging Techniques. Retin Cases Brief Rep. 2017; 11(Suppl 1):S178–S181. DOI: 10.1097/ICB.0000000000000419 [PubMed: 27599108]
20. Jayasundera T, Branham KEH, Othman M, Rhoades WR, Karoukis AJ, Khanna H, Swaroop A, Heckenlively JR. The RP2 Phenotype and Pathogenic Correlations in X-linked Retinitis Pigmentosa. Arch Ophthalmol. 2010; 128(7):915–923. DOI: 10.1001/archophthalmol.2010.122 [PubMed: 20625056]

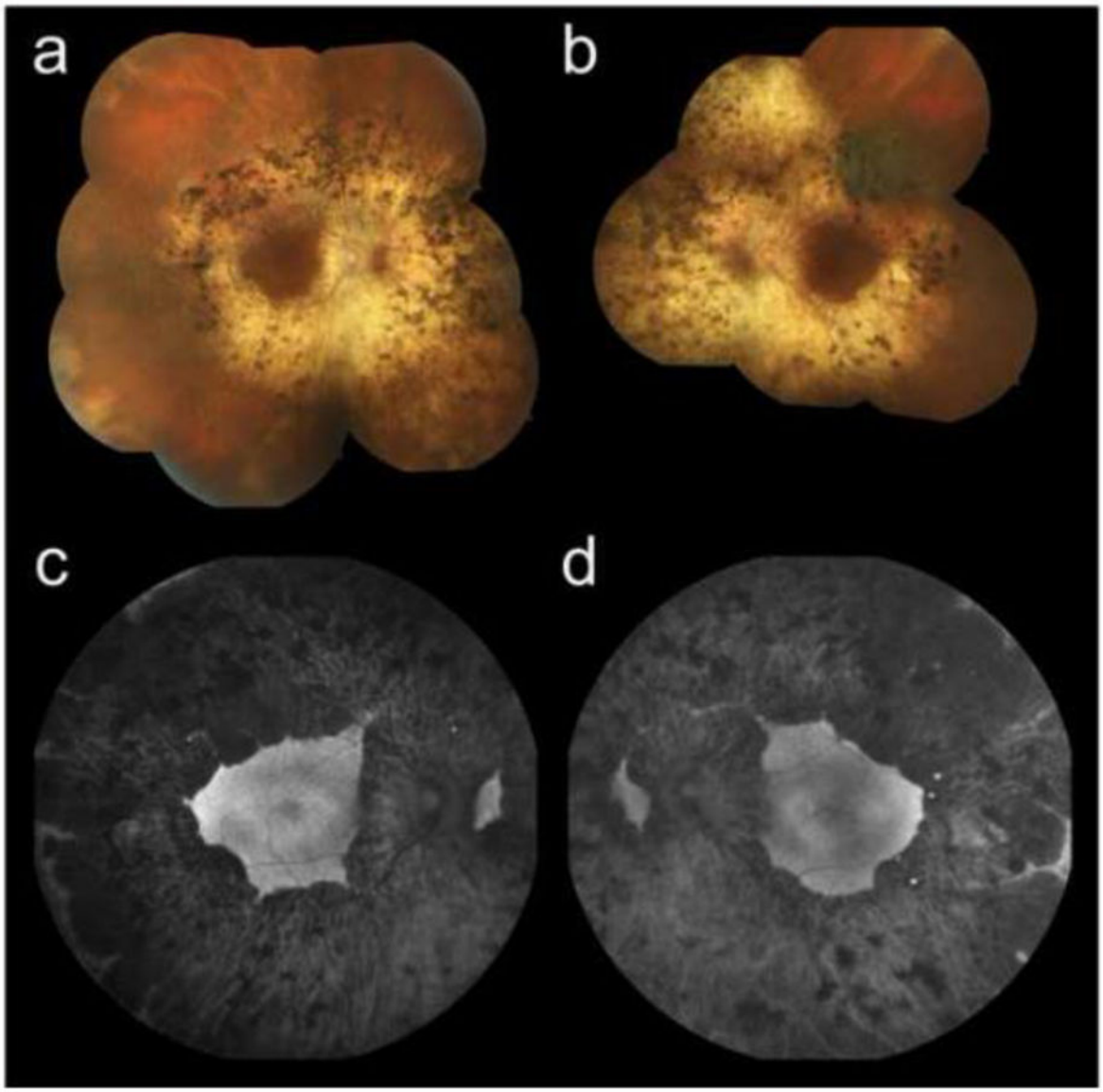

Fig. 1. Fundus and autofluorescent imaging characteristics of a SPATA7-RP patient at presentation

Digital color fundus photo of the right (a) and left (b) eyes showing extensive intraretinal pigment migration in the midperiphery, extensive atrophy of the RPE with choroidal sclerosis creating a pale appearance of the fundus. An island of spared RPE in the central maculae can be appreciated bilaterally, along with a small island nasal to the disc in both eyes. FAF imaging of the right (c) and left (d) eyes. Extensive hypoautofluorescent areas corresponding to RPE atrophy surround the centrally-spared islands, with sharp edges. The previously mentioned small RPE islands nasal to the discs in each eye can be appreciated more easily on autofluorescence and are relatively symmetric.

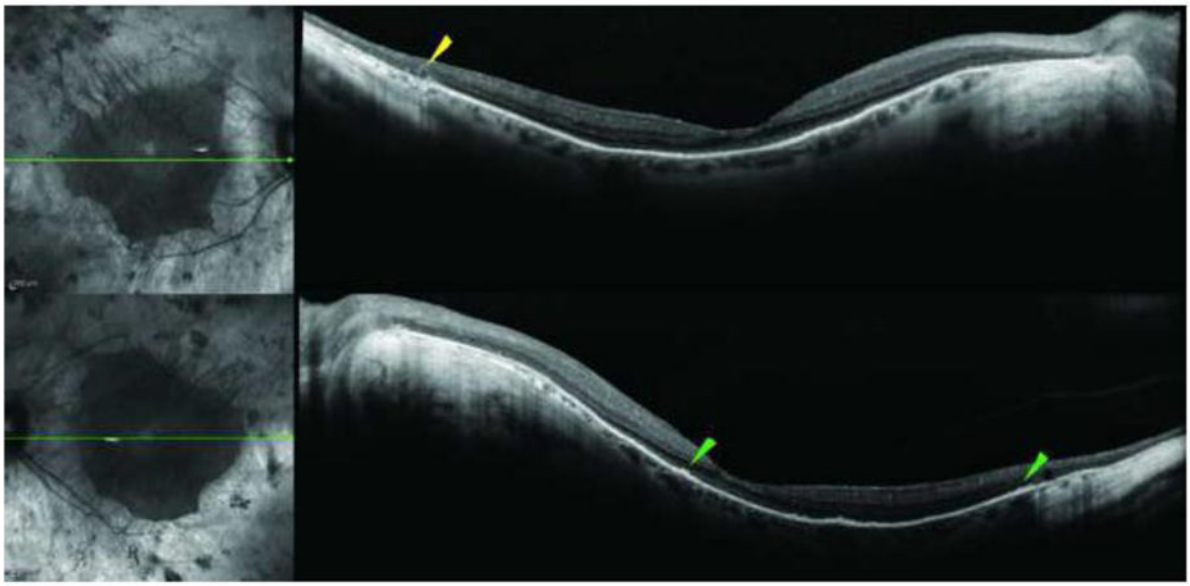

Fig 2. SD-OCT imaging through the fovea with concurrently registered infared images of a SPATA7-RP patient at presentation

In both the right (top row) and left (bottom row) eye, there is peripheral thinning of the ONL and extensive chorioretinal degeneration. RPE loss and chorodial sclerosis is evident outside the parafoveal region with increased transmittance of signal to the sclera. Green line, location of SD-OCT acquisition; green arrowhead, areas of RPE thickening.

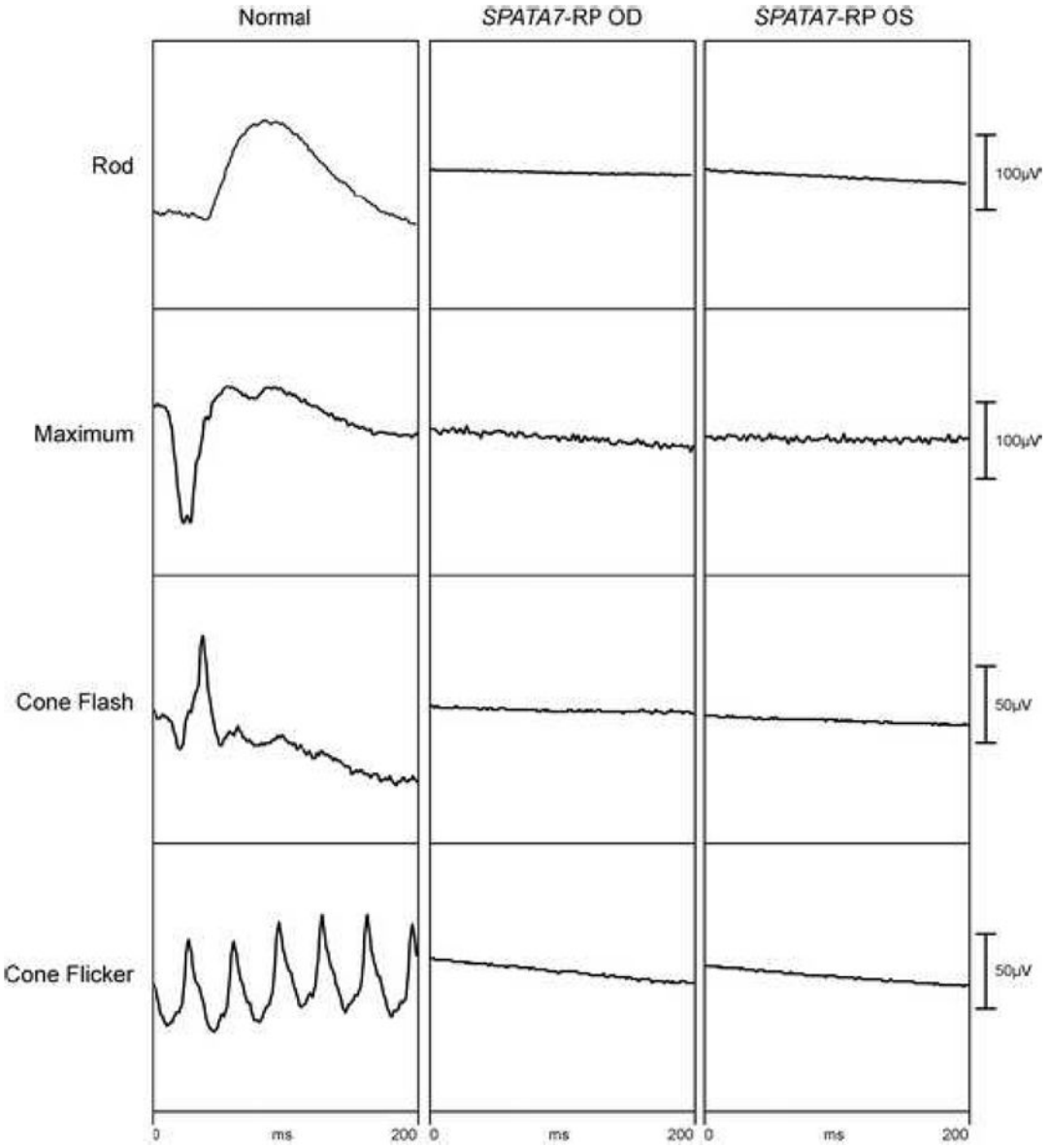

Fig 3. Full-field electroretinogram using DTL-recording electrodes of a SPATA7 patient at presentation compared to an age-matched normal patient

Scotopic rod-specific and maximum reponses were extinguished bilaterally. Photopic cone flash and 30 Hz-flicker were extinguished bilaterally.

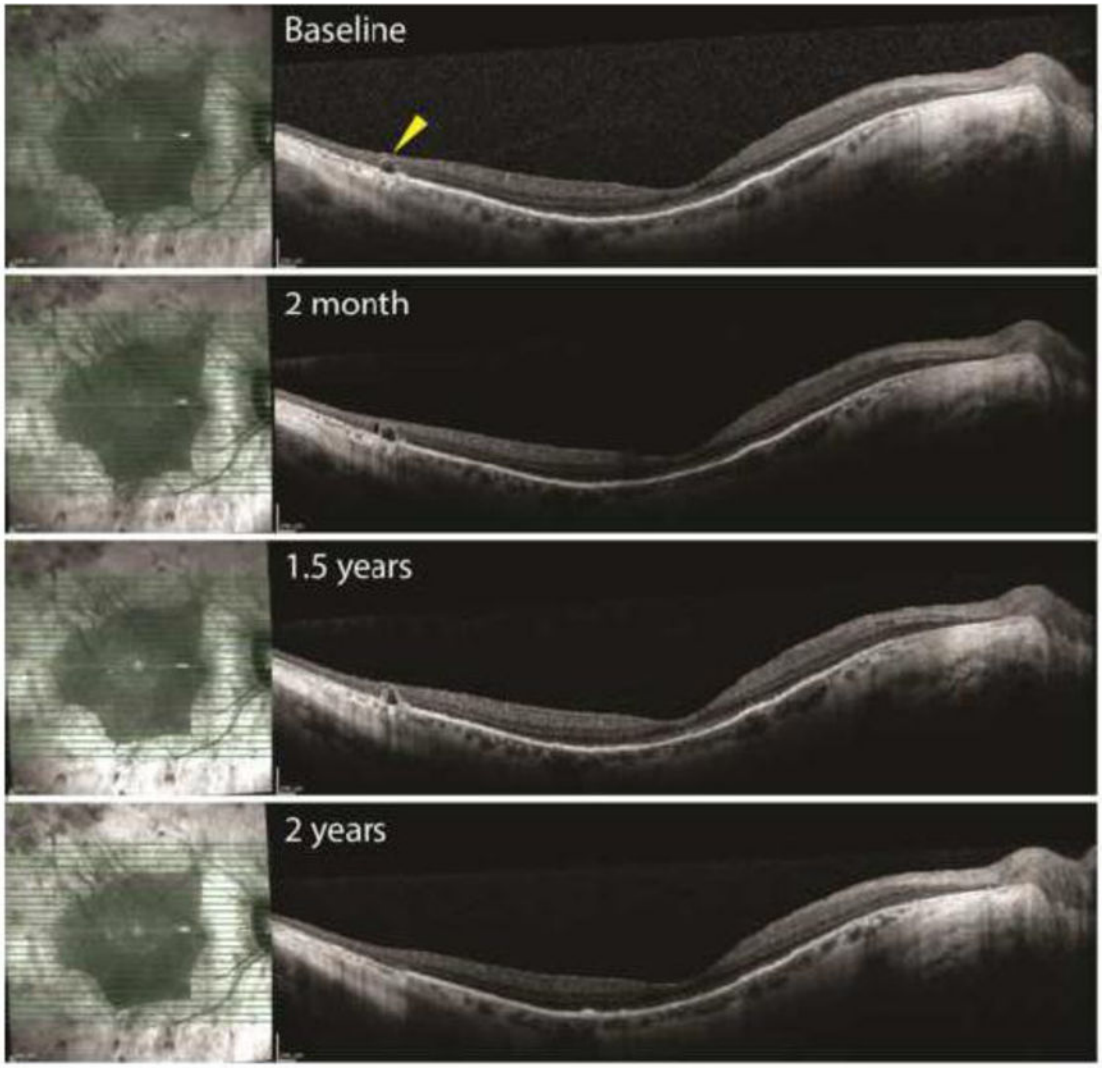

Fig 4. Serial SD-OCT imaging in the right eye of a SPATA7-RP patient

Outer retinal tubulation (ORT) was noted temporally in the right eye of the patient at baseline (top row). Serial imaging with the baseline image set as a reference, showed that that after two years there is RPE atrophy and increased choroidal sclerosis in the area of the previous ORT.

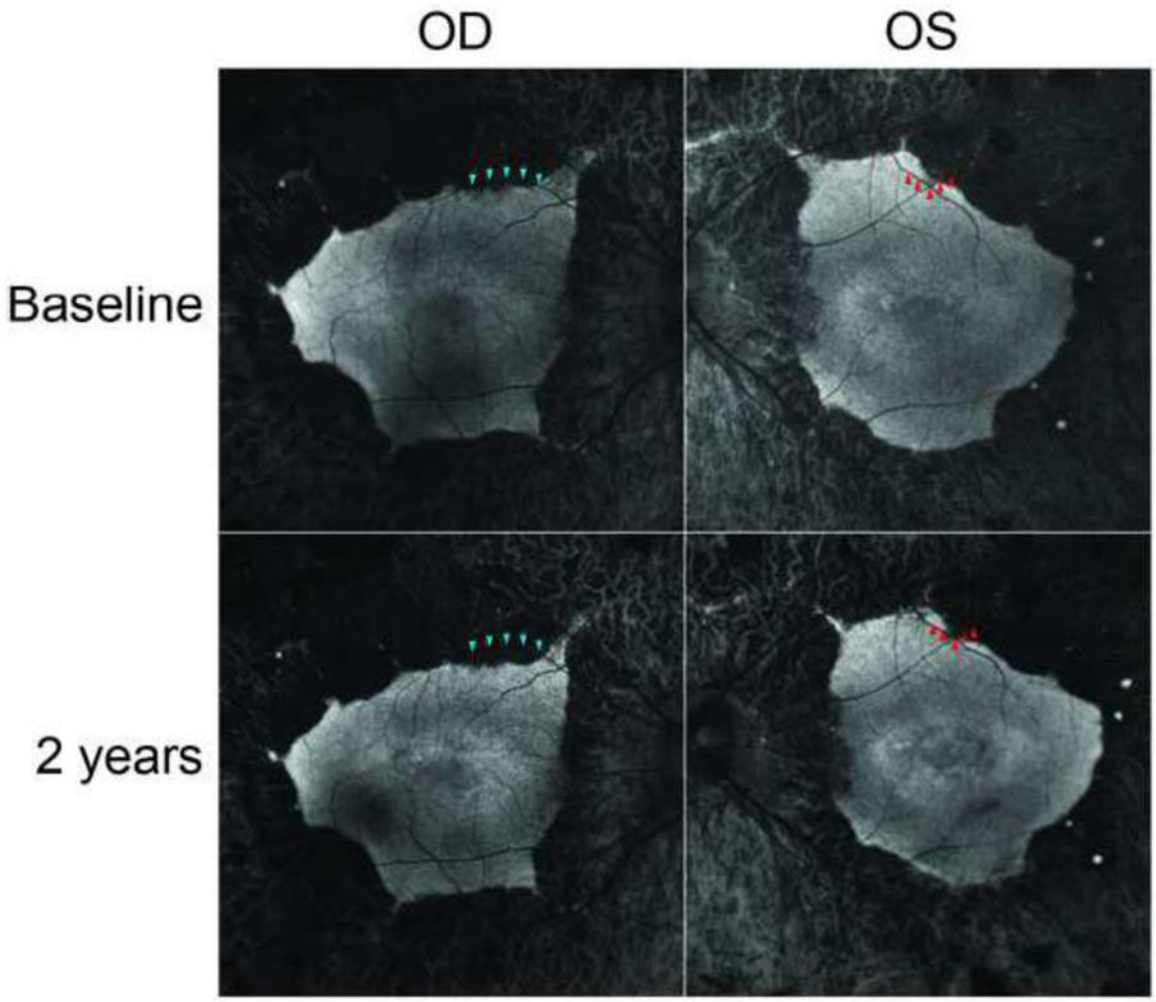

Fig 5. Progression of RPE atrophy seen over two years in a SPATA7-RP patient compared to baseline

An advancing edge of RPE atrophy is observed over two years of follow-up in the *SPATA7*-RP patient. Hypoautofluorescent areas represent marked RPE atrophy, revealing outlines of underlying choroidal vessels. Progression can be appreciated by comparing the location of atrophy in relation to vessels. An advancing edge is observable in the right and left eyes (blue and red triangles, respectively).

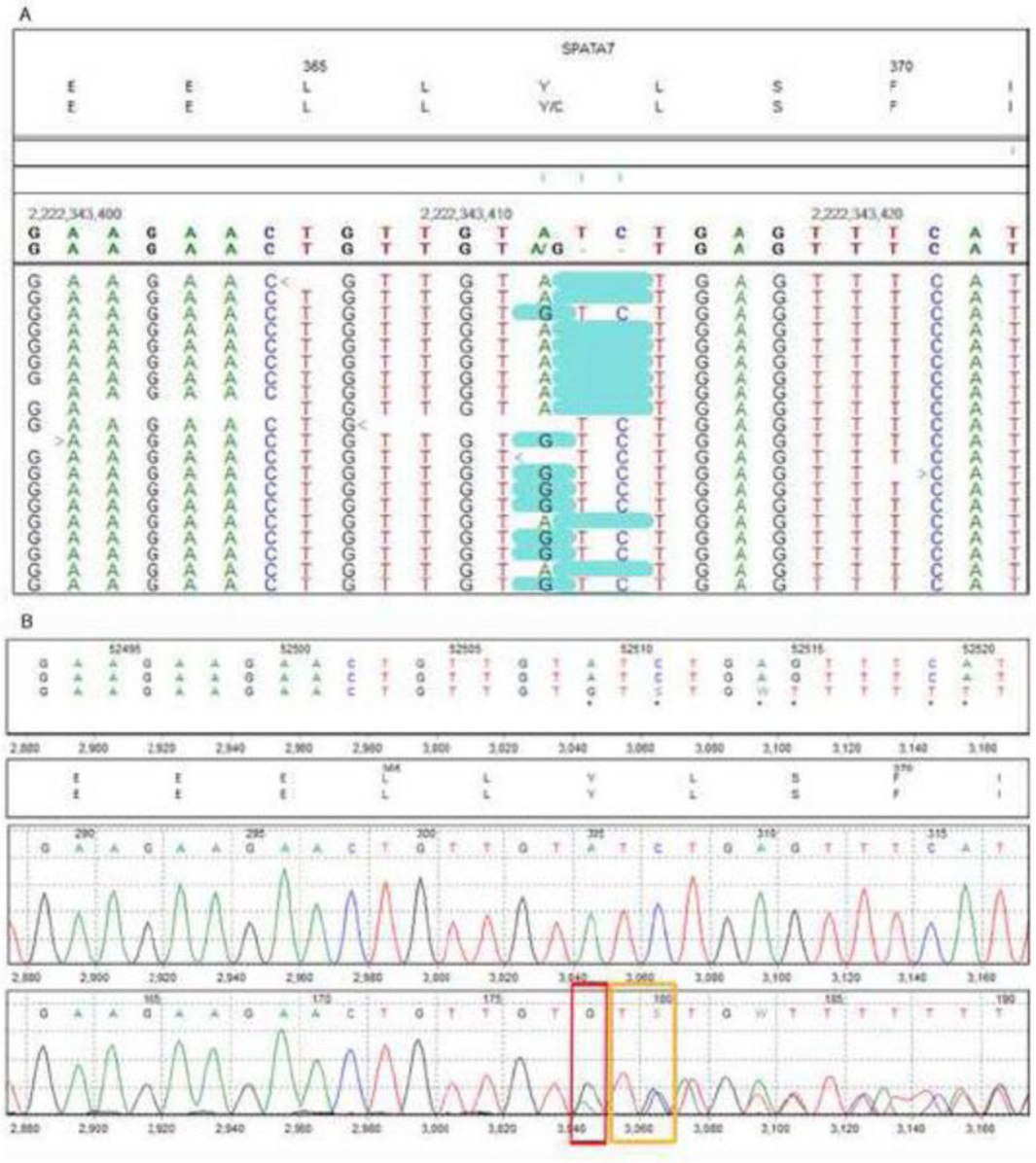

Fig. 6. Electropherogram

(a) Alignment of whole exome sequencing data in the *SPATA7* gene, with the reference sequence above, the patient reads below, and the changes highlighted in blue. In half the reads, there is an A to G change at base pair 1100 of the coding sequence resulting in a missense change from tyrosine to cysteine at position 367. The other half of the reads show a deletion of two base pairs (C and T) at position 1102 and 1103 resulting in a frameshift. Although these base pairs are part of the codons for tyrosine 367 and leucine 368, the first amino acid affected by the frameshift is leucine 368. Leucine is changed to glutamic acid with a premature stop codon four positions downstream. No reads contain both changes showing that these two mutations are in trans. (b) Sanger sequencing confirms both mutations in the patient. The top panels are the reference sequences and electropherogram

and the last panel is the electropherogram from the patient. Red box indicates the A to G change, the orange box indicates the deleted C and T base pairs.